JOURNAL OF PHYSIOLOGY AND PHARMACOLOGY 2014, 65, 5, 719-731
www.jpp.krakow.pl

A. CHELMONSKA-SOYTA[1,2], M. OZGO[3], A. LEPCZYNSKI[3], A. HEROSIMCZYK[3], K. BUSKA-PISAREK[1], A. KEDZIERSKA[1], D. NOWAK[4], A.J. MAZUR[4]

PROTEOME OF SPLEEN CD4 LYMPHOCYTES IN MOUSE PREIMPLANTATION PREGNANCY

[1]Laboratory of Reproductive Immunology, Ludwik Hirszfeld Institute of Immunology and Experimental Therapy, Polish Academy of Sciences, Wroclaw, Poland; [2]Faculty of Veterinary Medicine, Wroclaw University of Environmental and Life Sciences, Wroclaw, Poland; [3]Department of Physiology, Cytobiology and Proteomics, Faculty of Biotechnology and Animal Husbandry, West Pomeranian University of Technology, Szczecin, Poland; [4]Department of Cell Pathology, Faculty of Biotechnology, University of Wroclaw, Wroclaw, Poland

Pregnancy exerts profound impact on female immune system. The first signs of pregnancy recognition by immune system are observed even before implantation. The most visible effects are present in the local compartment, *i.e.* in uterine draining lymph nodes and the decidua, while peripheral changes are less obvious. In our recent paper we indicated that costimulation phenotype of APCs in spleens of female mice during the preimplantation period of pregnancy differs from mice in pseudopregnancy. However, the effect of differential costimulation in the context of the T lymphocyte function at periphery in early pregnancy is still unknown. For that reason, we decided to investigate global protein expression in splenic $CD4^+$ lymphocytes in order to identify and validate the most important biomarkers characteristic for the preimplantation period of pregnancy at periphery. Two-dimensional electrophoresis (2-DE) and mass spectrometry (MS) were utilized to analyze the protein expression pattern of magnetically sorted $CD4^+$ lymphocytes from spleens of pregnant and pseudopregnant females at 3.5 days after mating. The first goal of this study was to create a 2-DE map of the splenic $CD4^+$ T cells of pregnant mice. As a result, 106 protein spots from 373 were identified using MS. The comparison of lymphocyte protein patterns between pregnant and pseudopregnant mice depicted differential expression of 11 identified proteins belonging to the group of proteins involved in cytoskeletal structure, cell motility and metabolism. Profoundly diminished expression of cofilin-1, F-actin capping protein subunit alpha and malate dehydrogenase proteins in lymphocytes of pregnant mice indicates that preimplantation pregnancy could change the activation state of peripheral $CD4^+$ lymphocytes.

Key words: *$CD4^+$ lymphocytes, early pregnancy, proteome, spleen, mouse, antigen-presenting cells, cofilin-1*

INTRODUCTION

Regulatory mechanisms used by $CD4^+$ T lymphocytes place (T helper lymphocytes) these cells in the central position of a specific immune response. During pregnancy, these cells play a pivotal role in the maintenance of pregnancy. In mouse, an expansion of T_{reg} lymphocytes of $CD4^+CD25^+FOXP3^+$ phenotype in the uterine draining lymph nodes is clearly visible. Additionally, their depletion after allogenic matings is known to cause pregnancy failure (1). Likewise, the ratio of cytokines produced by Th1/Th2 lymphocytes at the feto-maternal interface is an indicator of successful or failing pregnancy (2).

On the other hand, the precise role of peripheral activity of $CD4^+$ lymphocytes in the context of pregnancy has not yet been determined. Recent papers have demonstrated that in humans not only production of Th1 type cytokines is decreased (3, 4), but also the overall adaptive immune response is weakened in favor of the innate immune mechanism protecting the mother from infectious antigens (5). In mice, the serum cytokine expression pattern during pregnancy is not clear (6), but an enlarged group of activated $CD4^+CD25^+$ spleen lymphocytes observed at early and more advanced stages of gestation suggests pregnancy-related regulation of peripheral immunity in this species (7, 8).

Our previous work indicated differential expression of costimulatory molecules on splenic antigen-presenting cells (APCs) within the first three days after mating in pregnant females in comparison to pseudopregnant mice. This data support the hypothesis of an early awareness of the immune system of the presence of paternal antigens (9). Exact effects of the mentioned phenomenon in the context of lymphocyte function are not clear. However, it may be assumed that APCs' specific phenotype during preimplantation pregnancy influences the activity of their counterparts - $CD4^+$ lymphocytes.

The proteomic approach has been successfully applied in studies aimed at examining the lymphocyte function in both physiological and pathological conditions (10, 11). The first gel-based proteomic reference map of T $CD4^+$ lymphocytes from non-

stimulated OVA-specific TCR transgenic male mice was created by Kaji *et al.* (12). From among 1300 detected protein spots, 255 proteins were identified. The human $CD4^+$ T lymphocyte activation-related proteome investigation performed by Lichtenfelds *et al.* (13) showed alterations in protein expression occurring in metabolism, cytoskeleton reorganization and modulation of signal transduction pathways dependent on the delivery of one or two activating signals. Moreover, identification and large-scale validation of differentially expressed proteins is possible in diseased conditions. The T lymphocyte proteomic analysis in patients with two hyperandrogenic syndromes, *i.e.* polycystic ovary syndrome and congenital adrenal hyperplasia, showed various protein expression in patients suffering from both diseases compared to healthy individuals. Additionally, exclusive protein expression characteristic for each of the examined diseases was characterized (14). It was also demonstrated that lymphocyte proteome changed during physiological pregnancy in sows. Peripheral blood mononuclear cells (PBMCs) were characterized using proteomic techniques during normal pregnancy at the 40^{th}, 70^{th} and 93^{rd} day of gestation. Differential expression of 93 proteins involved mainly in oxidative stress control in pregnant versus non-pregnant animals was observed (15).

To investigate the possible impact of the preimplantation process on the splenic lymphocytes, the present study included a proteomic analysis to assess the protein expression patterns of $CD4^+$ lymphocytes in pregnant and pseudopregnant mice. We established a proteomic map of $CD4^+$ lymphocytes of outbred CD1 mice at 3.5 days of pregnancy and identified differentially expressed proteins involved in cell migratory activity, cytoskeleton structure and metabolism in pregnant versus pseudopregnant mice.

MATERIAL AND METHODS

Animal preparation and material collection

All animal experiments were approved by the First Local Ethical Committee for Experiments on Animals at the Institute of Immunology and Experimental Therapy in Wroclaw No. 41/2010.

Outbred CD-1 mice were purchased from Charles Rivers Laboratories (Sulzfeld, Germany) and housed in a dark-light cycle (12:12) under SPF conditions. Two groups of 10 mice (4–6 weeks of age) were investigated. To equalize hormonal background in all females, mice were superovulated by intraperitoneal injection of 5 IU of pregnant mare serum gonadotropin (Folligon, Inervet, Poland) followed by 5 IU of human chorionic gonadotropin (Chorulon, Inervet, Poland) 46 hours later. Because hormones injection may interfere with the natural reproductive cycle, all females used in the experiments were in prepubertal age. Puberty was accelerated by the above- mentioned hormonal treatment and vaginal opening was confirmed by vaginal plug, and the presence of the embryos or oocytes in the lumen of the reproductive tract of mice indicated the induction of the first estrous cycle. Female mice from the control group (mice in pseudopregnancy) were mated with vasectomized males, while mice from the experimental group (pregnant mice) were mated with males with proven fertility. To minimize the putative impact of polymorphic seminal plasma antigens on female immune response, six and seven randomly chosen males were used in each group of mice respectively. Males' vasectomy was performed by surgical cut-off of 1 cm of each vas deferens under general anesthesia. The day of the vaginal plug confirmation was designated as 0.5 dpc. Vaginal plug inspection was done during morning hours (between 7.00–8.00 a.m.) after the night the females were mated. At 3.5 days of pregnancy/pseudopregnancy, mice were sacrificed and the uterus and spleen were dissected. The uterus was checked for the presence of embryos (pregnant mice) or oocytes (in pseudopregnant mice) by uterine flushings and microscopic examination.

$CD4^+$ T cells isolation and sorting

To obtain a single cell suspension of splenocytes, each spleen collected from mice was squeezed through the cell strainer to the ammonium chloride solution to enable erythrocytes lysis. Splenocytes were labeled using a $CD4^+$ T cell isolation kit (Miltenyi Biotec, USA) following modified manufacturer instructions. Briefly, splenocytes were stained with a cocktail of biotin-conjugated antibodies against CD8 , CD11b, CD11c, CD19, CD45R (B220), CD49b (DX5), CD105, anti-MHC-class II, and Ter-119, subsequently magnetically labeled with anti-biotin microbeads for depletion. Due to the required need of higher purity of the sorted population, no more than 40×10^6 splenocytes were added to the MS separation column. Purity of isolated cells was confirmed by flow cytometry analysis by staining with anti-mouse CD4 FITC antibody (eBioscience, Vienna, Austria). The average purity of sorted cells was 82.75 ± 5.09% of CD4 positive cells among all isolated lymphocytes. The average concentration of isolated cells was $3.5\times10^6 \pm 2.45$ ($1.0\text{-}9.5\times10^6$ cells per sorting).

2D electrophoresis sample preparation

The sorted cells were later resuspended in the lysis buffer containing 2 M thiourea (Sigma, St. Louis, USA), 5 M urea (Sigma), 4% CHAPS (Bio-Rad), 0.2% Biolyte (Bio-Rad, USA), 40 mM Tris (Sigma), 1:100 Protease Inhibitor Cocktail 3 (Calbiolchem, USA). The samples were incubated for 30 minutes on ice (4°C) and sonicated twice for 30 seconds. After the sonication, the cell suspension was incubated (30 min, on ice), centrifuged (4°C, 15 min, 13,000×g) and stored at –80°C until further analysis.

Two-dimensional electrophoresis (2-DE)

Due to the low protein content, samples from 10 mice in each group were pooled to the final number of 6 in each group. The samples were precipitated with ice-cold acetone for 2 hours at –20°C. Protein pellets were dissolved in the lysis buffer (5 M urea, 2 M thiourea, 4% w/v CHAPS, 40 mM Tris, 0.2% w/v 3-10 ampholytes (Bio-Rad) and 2 mM TBP (Bio-Rad)). Analytical gels were obtained with 70 µg total protein load and preparative gels with 200 µg protein load. Analytical gels were used for image analysis and preparative gels for spot extraction and MS identification. The first dimension was run (Protean® IEF Cell, Bio-Rad) using 4-7, 17 cm NL ReadyStrip™ IPG Strips (Bio-Rad) in total 90 000 Vh. Prior to the second dimension SDS-PAGE, focused IPG strips were reduced with DTT (Sigma) in equilibration buffer (6 M urea, 0.5 M Tris/HCl, pH 6.8, 2% w/v SDS, 30% w/v glycerol and 1% w/v DTT) and alkylated with iodoacetamide (2.5% w/v). After equilibration, strips were placed on the top of 12% SDS polyacrylamide gels (25×20 cm) and held with molten 0.5% (w/v) agarose. SDS-PAGE was run in a Protean Plus™ Dodeca Cell™ electrophoretic chamber (Bio-Rad) at 40 V for 1 hour and subsequently at 90V for 15 hours at 10°C. After 2-DE separation, analytical gels were visualized with silver stain according to Chevallet *et al.* (16) and preparative gels with colloidal Coomassie Brilliant Blue G-250 according to the Hoving protocol (17).

Image analysis

Gels were scanned using a GS-800™ Calibrated Densitometer (Bio-Rad). The 2-D image analysis was performed using PDQuest

Analysis software version 8.0 Advanced (Bio-Rad). To measure the intragroup variability, the coefficient of variation (CV%) for each replicate group was calculated. The between-group qualitative and quantitative comparison was performed to show the differences in the protein spots pattern between the groups and to examine the changes in the protein expression level. Importance of protein expression pattern changes was confirmed by Student's t-test. Experiment normalization was conducted using a local regression model (LOESS). On the basis of a molecular range standard, observed molecular mass (kDa) was computed for each identified protein spot.

Mass spectrometry

Protein spots were manually excised from Coomassie stained gels and were decolorized by washing with buffer (25 mM NH_4HCO_3 in 5% v/v ACN) followed by two washes with a solution containing 25 mM NH_4HCO_3 in 50% v/v ACN. The excised gel pieces were dehydrated (100% ACN), vacuum dried and incubated with trypsin (20 µl/spot of 12.5 µg/ml in 25 mM NH_4HCO_3; Sigma) for 16 hours at 37°C. The resulting peptides were extracted with 100% ACN, combined with an equal volume of matrix solution (5 mg/ml CHCA, 0.1% v/v TFA, 50% v/v ACN) and loaded onto a MALDI-MSP AnchorChip™ 600/96 plate (Bruker Daltonics, Germany). For calibrating the mass scale, peptide mass standard II (Bruker Daltonics, Germany within mass range 700-3200 Da) was used. Mass spectra were acquired in the positive-ion reflector mode using a Microflex™ MALDI TOF mass spectrometer (Bruker Daltonics, Germany). The PMF (peptide mass fingerprinting) data were compared to mammalian databases (SWISS-PROT; http://us.expasy.org/uniprot/) with the aid of MASCOT search engine (19) (http://www.matrixscience .com/). Search parameters were trypsin - as an enzyme, carbamidomethylation of cystein - as fixed modification, methionine oxidation - as variable modification, mass tolerance to 150 ppm, a maximum of one missed cleavage site. On this basis, the achieved results were further validated by the MASCOT score (only statistically significant hits were applied) and sequence coverage.

To define the subcellular localization of the identified proteins, a bioinformatics tool was employed - Euk-mPLoc 2.0 (http://www.csbio.sjtu.edu.cn/bioinf/euk-multi-2/).

RESULTS

2-DE gel proteome map of the splenic CD4 positive T cells

The first goal of this study was to introduce a 2-DE and MALDI-TOF MS based proteomic workflow to demonstrate, protein profile of the splenic CD4 positive T cells of pregnant and pseudopregnant mice. Afterwards, the comparison of splenic CD4 cells protein profiles was performed to investigate preimplantation pregnancy characteristic protein pattern. The resulting map of splenic $CD4^+$ T lymphocyte of pregnant mice revealed 373 ± 30 protein spots with a molecular weight between 10 and 120 kDa and pIs between 4 and 7, which is presented in *Fig. 1*. The analysis showed that spot locations and stain intensities on the 2-D gels were similar between the gels from the different samples. All protein spots were excised from the gels and submitted for identification by peptide mass fingerprinting using MALDITOF MS. On this basis, a total of 106 spots (identification rate of 28.42%) were successfully identified, representing 63 distinct gene products. The results of the MALDI-TOF MS analyses are summarized in *Table 1*. The analysis of intragroup variation for each protein spot showed an average CV for replicate groups, respectively, for pregnant mice 39.12% and for pseudopregnant mice 54.19%. Names and other details of the identified proteins are listed in *Table 1* according to SWISS-PROT database. Detailed properties and functions of the identified proteins are listed in *Table 2*.

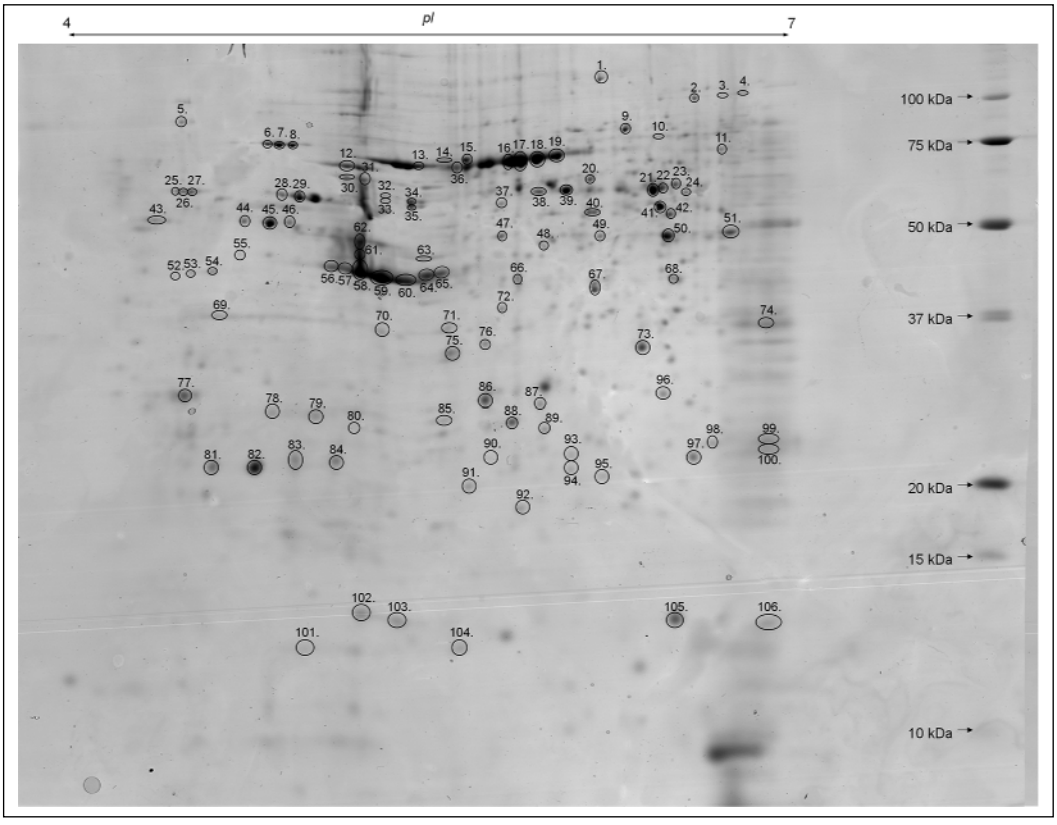

Fig. 1. Representative two-dimensional map of splenic CD4 positive T cells proteins. 2-D gel presents Coomassie-stained protein pattern (800 µg of proteins, 4-7 NL IPG, 12% SDS-PAGE). Spot numbers refer to the numbers in *Table 1*.

Among the identified proteins, 21 were expressed as a multiple spots, demonstrating that they are isoforms, whereas the resulting 42 proteins were resolved as a single spots. The smallest molecular masses (Mr) of the identified splenic CD4 positive T cell proteins are assigned to both the glyoxalase domain-containing protein 4 (12.10 kDa) and ATP synthase subunit d (12.10 kDa), whereas the largest is attributed to vinculin (114.20 kDa).

Subcellular distribution of proteins showed that 39.61% of the 106 protein spots were classified as cytoplasmic (CY), 21.70% as cytoskeletal (CS), 13.21% as mitochondrial (MT) and 10.38% as nuclear (NU) proteins. The remaining 15% were assigned to lysosomal (LY, 2.83%), membranous (CM, 1.89%), centrosomal (CE, 0.94%) and extracellular (ECR, 1.89%) proteins. To take a qualitative overview of the expressed splenic

Table 1. Summary of protein identification from splenic CD4 positive T cells of pregnant mice.
Abbreviations: MT - mitochondria, CY - cytoplasm, CM - cell membrane, ER - endoplasmic reticulum, NU - nucleus, CE - centrosome, CS - cytoskeleton, ECR - extracellular region, LY - lysosomes, # - protein present in proteomic map of $CD4^+$ T lymphocytes (Kaji *et al.*, *Electrophoresis* 2003; 24: 2433), E - estrogen regulated expression , ns- estrogen regulated expression not shown according to PubMed database. A reference list for estrogen related expression of identified proteins is attached in *Table 3*.

Spot No.	Short name	Description	Accession number	MALDI-TOF MS		Theoretical pI/ M_r [pH/kDa]	Observed M_r [kDa]	Subcellular localization
				Peptides matched	Sequence coverage (%)			
Metabolism								
89	PNP	Purine nucleoside phosphorylase	P23492	13	48	5.78/32.54	24.40	CY; #; ns
99	CA-II	Carbonic anhydrase 2	P00920	10	56	6.49/29.13	23.60	CY; E
100	CA-I	Carbonic anhydrase 1	P13634	7	50	6.44/28.37	22.80	CY; E
67	LEI-A	Leukocyte elastase inhibitor A	Q9D154	6	16	5.85/42.72	40.90	CY; ns
49	H2A.1-H	Histone H2A type 1-H	Q8CGP6	8	69	11.03/13.94	48.30	NU; E
85	UMP-CMPK	UMP-CMP kinase	Q9DBP5	6	37	5.68/22.38	25.30	CY; E
92				6	37		18.20	
Energy								
Glycolysis and gluconeogenesis								
50	ENO1	Alpha-enolase	P17182	22	59	6.37/47.45	48.30	CY; #; E
51				16	44		48.90	
71	PDHE1-B	Pyruvate dehydrogenase E1 component subunit beta, mitochondrial	Q9D051	9	27	6.41/39.25	35.30	MT; #; ns
74	GAPDH	Glyceraldehyde-3-phosphate dehydrogenase	Q569X5	11	46	8.44/36.07	35.70	CY; E
Pentose-phosphate pathway								
23	G6PD	Glucose-6-phosphate 1-dehydrogenase X	Q00612	13	35	6.06/59.68	61.10	CY; #; ns
Respiration and fermentation								
42	ALDHI	Aldehyde dehydrogenase, mitochondrial precursor	P47738	15	39	7.53/57.01	53.10	MT; ns
73	MDH	Malate dehydrogenase, cytoplasmic	P14152	10	33	6.16/36.66	33.00	CY; #; ns
72	IDH3A	Isocitrate dehydrogenase subunit alpha, mitochondrial precursor	Q9D6R2	12	31	6.27/40.07	37.90	MT; #; ns
44	ATP5B	ATP synthase subunit beta, mitochondrial precursor	P56480	23	51	5.19/56.26	51.20	MT; #; E
45				30	62		50.50	
46				13	35		50.80	
104	ATP5H	ATP synthase subunit d, mitochondrial	Q9DCX2	13	76	5.52/18.79	12.10	MT; #; E
Cellular organisation								
Cytoskeleton - cell structure								
1	VINC	Vinculin	Q64727	11	13	5.77/117.21	114.20	CS; E
9	EZRI	Vinculin	P26040	15	27	5.83/69.48	81.70	CY; #; E
11				15	20		72.60	
77	TPM3	Tropomyosin alpha-3 chain	P21107	9	21	4.68/32.90	27.60	CS; #; E
43	COF1	Cofilin-1	P18760	10	57	8.22/18.78	51.40	CY; ns
105				6	62		13.00	
Cytoskeleton - cell motility								
21	COR1A	Coronin-1A	O89053	16	39	6.05/51.64	59.40	CS; #; ns
22				10	32		60.00	
31	ACTB	Actin, cytoplasmic 1	P60710	25	65	5.29/41.74	62.30	CS; #
55				18	43		45.20	
56				23	54		43.60	
57				26	54		43.60	
58				22	52		42.60	
59				12	51		42.00	
60				15	51		41.70	
61				11	50		44.40	
64				19	51		42.30	
65				18	63		42.70	
66				8	31		42.00	
79				7	30		25.70	
78	ACTG	Actin, cytoplasmic 2	P63260	10	44	5.31/42.11	26.10	CS; #; E
70	CAPZA1	F-actin-capping protein subunit alpha-1	P47753	10	46	5.34/33.09	35.00	CS; #; E
76	CAPZA2	F-actin-capping protein subunit alpha-2	P47754	5	29	5.57/33.12	33.40	CS; #
86	CAPZB	F-actin-capping protein subunit beta	P47757	8	24	5.47/31.61	27.20	CS; #
87				12	39		26.70	
37	ARP3	Actin-like protein 3	Q99JY9	10	42	5.61/47.78	55.70	CS; #
106				8	23		12.90	
Cytoskeleton - intermediate filament family								
28	VIME	Vimentin	P20152	16	40	5.06/53.71	58.20	CY; #; ns

29				29	59		57.50	
12	LMNB1	Lamin-B1	P14733	40	61	5.11/66.97	66.90	NU; #; ns
95	TMEM43	Transmembrane protein 43	Q5XIP9	7	17	6.85/44.86	20.60	CM; ns
Cell cycle								
2	PDC6I	Programmed cell death 6-interacting protein	Q9WU78	26	33	6.15/96.52	99.70	CY; ns
13	hnRNP K	Heterogeneous nuclear ribonucleoprotein K	P61979	13	33	5.39/51.23	67.20	NU; #; E
30				17	35		63.30	
80	PHB	Prohibitin	P67778	11	60	5.57/29.86	24.70	MT; E
69	NPM	Nucleophosmin	Q61937	9	34	4.62/32.71	37.00	CE; E
Protein turnover								
Transcription and protein synthesis								
52	RPSA	40S ribosomal protein SA	P14206	11	51	4.80/32.93	42.70	CY; ns
53				6	31		42.90	
54				11	51		43.00	
3	EF2	Elongation factor 2	P58252	17	29	6.41/96.22	102.20	CY; #; E
4				19	29		103.30	
24	PRPF19	Pre-mRNA-processing factor 19	Q99KP6	6	17	6.14/55.66	58.90	NU; ns
40	hnRNP H	Heterogeneous nuclear ribonucleoprotein H	O35737	8	22	5.89/49.45	53.50	NU; E
68	hnRNP A/B	Heterogeneous nuclear ribonucleoprotein A/B	Q99020	7	23	7.68/30.93	41.80	NU; E
Protein degradation								
96	PSMA1	Proteasome subunit alpha type-1	Q9R1P4	8	28	6.00/29.81	27.80	CY; ns
98	PSMA6	Proteasome subunit alpha type-6	Q9QUM9	7	33	6.34/27.81	23.20	NU; ns
91	PSMB4	Proteasome subunit beta type-4 precursor	P99026	5	25	5.47/29.21	19.80	NU; #; ns
88	PSME1	Proteasome activator complex subunit 1	P97371	14	59	5.73/28.83	25.10	CY; #; ns
36	CATH	Cathepsin H precursor	P49935	7	27	8.68/37.73	66.40	LY; E
Protein folding and modification								
25	PDIA1	Protein disulfide-isomerase precursor	P09103	26	51	4.79/57.51	59.30	ER; #; ns
26				15	31		59.10	
27				12	25		59.00	
39				19	44		59.30	
38	PDIA3	Protein disulfide-isomerase A3 precursor	P27773	26	53	5.88/57.09	59.00	ER; ns
20	TCPA1	T-complex protein 1 subunit alpha A	P11984	10	25	5.76/60.93	62.80	CY; ns
41	TCPB	T-complex protein 1 subunit beta	P80314	26	60	5.97/57.78	54.40	CY; ns
16	TCPQ	T-complex protein 1 subunit theta	P42932	14	40	5.44/60.09	68.10	CY; ns
17				15	39		68.50	
18				13	34		69.00	
19				13	35		70.30	
10	HSP7C	Heat shock cognate 71 kDa protein	P63017	32	56	5.37/71.05	77.60	NU; #; ns
6	GRP78	78 kDa glucose-regulated protein precursor	P20029	24	40	5.07/72.49	74.50	ECR; E
7				32	49		74.10	
8				34	49		74.10	
Signal transduction								
94	GRB2	Growth factor receptor-bound protein 2	Q60631	11	41	5.89/25.34	21.10	CY; E
75	ANXA3	Annexin A3	O35639	13	41	5.33/36.52	32.30	CY; ns
84	GDIR1	Rho GDP-dissociation inhibitor 1	Q99PT1	10	54	5.12/23.45	21.70	CY; #; E
81	GDIR2	Rho GDP-dissociation inhibitor 2	Q61599	5	42	4.97/22.89	21.30	CY; #; E
82				6	54		21.20	
83				9	69		21.80	
102				9	60		13.10	
103				7	59		12.90	
5	HCLS1	Hematopoietic lineage cell-specific protein	P49710	16	33	4.73/54.24	85.60	NU; #; ns
Cell protection, defence and stress								
93	PRDX6	Peroxiredoxin-6	O08709	9	53	5.71/24.97	22.30	LY; ns
97				12	60		22.10	
32	CH60	60 kDa heat shock protein, mitochondrial precursor	P63038	15	33	5.91/61.09	57.80	MT; E
33				16	39		56.60	
34				17	47		56.10	
35				17	35		54.70	
14	GRP75	Stress-70 protein, mitochondrial precursor	P38647	19	28	5.91/73.77	68.60	MT;#;ns
15				25	40		68.90	
101	GLOD4	Glyoxalase domain-containing protein 4	Q9CPV4	10	35	5.28/33.58	12.10	CY; #; ns
Immunological defence								
47	IGHA1	Ig alpha-1 chain C region	P01876	9	25	6.08/38.49	48.30	ECR; E
62	S10A9	Protein S100-A9	P31725	9	44	6.64/13.21	47.40	CY; ns
63				7	42		44.90	
90	FRIL1	Ferritin light chain 1	P29391	5	36	5.66/20.85	21.90	ECR; ns
Other								
48	MFA3L	Microfibrillar-associated protein 3-like	Q9D3X9	10	21	5.00/45.77	46.80	CM

CD4 positive T cell proteins of pregnant mice, the identified proteins were categorized into 8 groups based on their known functions (*Table 1*). These proteins are involved in cellular organization (33.96%), protein turnover (26.42%), energetic processes (11.32%), cell protection, defense and stress (8.49%), signal transduction (8.49%), immunological defense (3.78%), metabolism (6.6%) and other functions (0.94%).

Differentially expressed proteins

$CD4^+$ lymphocytes samples from pregnant (n=6) and pseudopregnant (n=6) mice were processed in duplicate (24 gels in total). Using bioinformatics software, we found that 25 protein spots were significantly altered when compared to the control group (*Fig. 2*). Among these spots, 13 were up-regulated and the

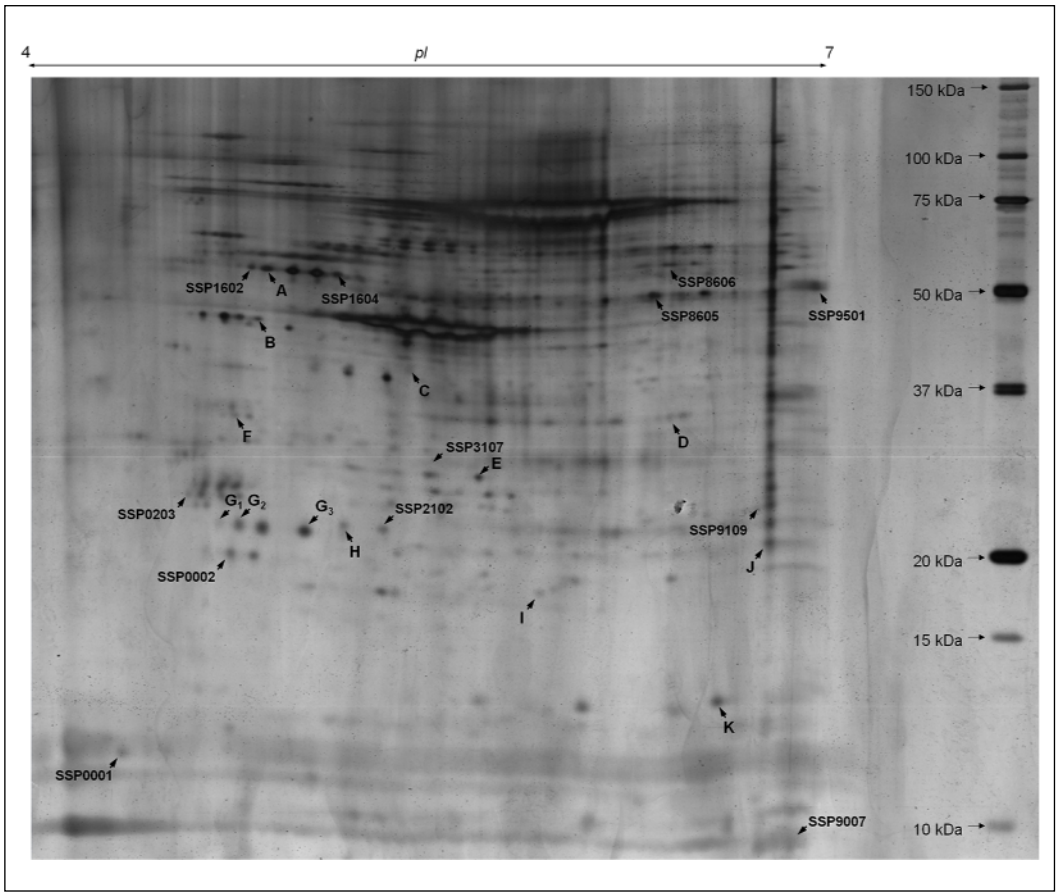

Fig. 2. Representative two-dimensional map of splenic CD4 positive T cells proteins. 2-D gel presents silver-stained protein pattern (70 µg of proteins, 4-7 NL IPG, 12% SDS-PAGE). Letters (A-K) and SSP numbers refer to significantly altered proteins described in details in *Table 2*.

Table 2. List of differentailly expressed proteins of splenic CD4 positive T cells between pseudopregnant and pregnant mice.

Spot	Protein name	Short name	Average abundance (pseudo-pregnancy)	S.D.	Average abundance (pregnancy)	S.D.	Fold regulation	Significance of differences	Protein properties and function
A	ATP synthase subunit beta E	ATP5B	**297.10**	*19.25*	**623.52**	*73.30*	2.10	P≤0.05	Mitochondrial membrane ATP synthase (F_1F_0 ATP synthase or Complex V) produces ATP from ADP in the presence of a proton gradient across the membrane which is generated by electron transport complexes of the respiratory chain. F-type ATPases consist of two structural domains, F_1 - containing the extramembraneous catalytic core, and F_0 - containing the membrane proton channel, linked together by a central stalk and a peripheral stalk. During catalysis, ATP synthesis in the catalytic domain of F_1 is coupled *via* a rotary mechanism of the central stalk subunits to proton translocation. Subunits alpha and beta form the catalytic core in F_1. Rotation of the central stalk against the surrounding $alpha_3beta_3$ subunits leads to hydrolysis of ATP in three separate catalytic sites on the beta subunits (47, 48).
B	40S ribosomal protein	RPSA	**253.42**	*35.33*	**168.65**	*33.89*	–1.50	P≤0.05	May play an important role in controlling cell growth and proliferation through the selective translation of particular classes of mRNA (49,50).
C	F-actin capping protein subunit alpha-1E	CAPZA1	**520.07**	*58.45*	**208.10**	*26.42*	–2.50	P≤0.05	F-actin-capping proteins bind in a Ca2+-independent manner to the fast growing ends of actin filaments (barbed end) thereby blocking the exchange of subunits at these ends. Unlike other capping proteins (such as gelsolin and severin), these proteins do not sever actin filaments (51).
D	Malate dehydrogenase, cytoplasmic	MDH	**692.87**	*37.44*	**96.45**	*1.91*	–7.19	P≤0.01	L-malate dehydrogenase plays a crucial role in many important metabolic pathway including the tricarboxylic acid cycle, glyoxylate bypass, amino

									acid synthesis, gluconeogenesis and facilitation of exchange of metabolites between cytoplasm and subcellular organelles (52, 53).
E	F-actin capping protein subunit alpha-2	CAPZA2	**240.90**	*45.28*	**38.20**	*2.40*	–6.31	P≤0.05	F-actin-capping proteins bind in a Ca2+-independent manner to the fast growing ends of actin filaments (barbed end) thereby blocking the exchange of subunits at these ends. Unlike other capping proteins (such as gelsolin and severin), these proteins do not sever actin filaments (51).
F	Tropomyosin alpha-3 chain E	TPM3	**59.70**	*15.32*	**144.32**	*38.50*	2.42	P≤0.01	Binds to actin filaments in muscle and non-muscle cells. Plays a central role, in association with the troponin complex, in the calcium dependent regulation of vertebrate striated muscle contraction. Smooth muscle contraction is regulated by interaction with caldesmon. In non-muscle cells is implicated in stabilizing cytoskeleton actin filaments (54).
G_1	Rho GDP-dissociation inhibitor 2 E	GDIR2	**85.40**	*12.12*	**224.50**	*63.95*	2.63	P≤0.01	Regulates the GDP/GTP exchange reaction of the Rho proteins by inhibiting the dissociation of GDP from them, and the subsequent binding of GTP to them (55).
G_2			**270.60**	*46.04*	**505.65**	*65.35*	1.87	P≤0.01	
G_3			**693.00**	*60.10*	**1087.20**	*289.81*	1.57	P≤0.01	
H	Rho GDP-dissociation inhibitor 1E	GDIR1	**269.05**	*19.59*	**104.23**	*5.62*	–2.58	P≤0.05	Controls Rho proteins homeostasis. Regulates the GDP/GTP exchange reaction of the Rho proteins by inhibiting the dissociation of GDP from them, and the subsequent binding of GTP to them. Retains Rho proteins such as CDC42, RAC1 and RHOA in an inactive cytosolic pool, regulating their stability and protecting them from degradation. Actively involved in the recycling and distribution of activated Rho GTPases in the cell, mediates extraction from membranes of both inactive and activated molecules due its exceptionally high affinity for prenylated forms (56).
I	Proteasome subunit beta type-4	PSMB4	**259.27**	*87.12*	**98.27**	*24.76*	–2.64	P≤0.05	The proteasome is a multicatalytic proteinase complex which is characterized by its ability to cleave peptides with Arg, Phe, Tyr, Leu, and Glu adjacent to the leaving group at neutral or slightly basic pH. The proteasome has an ATP-dependent proteolytic activity (57).
J	Carbonic anhydrase 2 E	CA-II	**494.68**	*142.15*	**890.35**	*265.02*	1.80	P≤0.05	Essential for bone resorption and osteoclast differentiation. Reversible hydration of carbon dioxide. Contributes to intracellular pH regulation in the duodenal upper villous epithelium during proton-coupled peptide absorption. Stimulates the chloride-bicarbonate exchange activity of SLC26A6 (58).
K	Cofilin-1	COF1	**905.85**	*244.73*	**220.37**	*81.16*	–4.11	P≤0.01	Binds to F-actin and exhibits pH-sensitive F-actin depolymerizing activity. Regulates actin cytoskeleton dynamics. Plays a role in the regulation of cell morphology and cytoskeletal organization. Required for the up-regulation of atypical chemokine receptor ACKR2 from endosomal compartment to cell membrane, increasing its efficiency in chemokine uptake and degradation (59).
SSP 0001	Not identified		**271.80**	*26.61*	**87.40**	*11.78*	–3.11	P≤0.05	
SSP 0002	Not identified		**199.82**	*26.62*	**276.45**	*38.00*	1.38	P≤0.01	
SSP 0203	Not identified		**113.52**	*55.12*	**243.22**	*17.71*	2.14	P≤0.01	
SSP 1602	Not identified		**313.30**	*118.37*	**404.20**	*46.49*	1.29	P≤0.05	
SSP 1604	Not identified		**297.10**	*19.25*	**623.52**	*73.30*	2.10	P≤0.05	
SSP 2102	Not identified		**610.67**	*155.80*	**178.20**	*47.30*	–3.43	P≤0.01	
SSP 3107	Not identified		**24.95**	*3.76*	**77.80**	*14.62*	3.12	P≤0.01	
SSP 8605	Not identified		**317.05**	*111.54*	**540.42**	*128.72*	1.70	P≤0.05	
SSP 8606	Not identified		**504.35**	*117.02*	**90.80**	*49.37*	–5.55	P≤0.01	
SSP 9007	Not identified		**1091.57**	*227.87*	**692.40**	*158.49*	–1.58	P≤0.05	

SSP 9101	Not identified	**855.67**	*137.40*	**302.95**	*22.27*	–2.82	P≤0.01
SSP 9501	Not identified	**659.22**	*111.84*	**1155.55**	*425.92*	1.75	P≤0.05

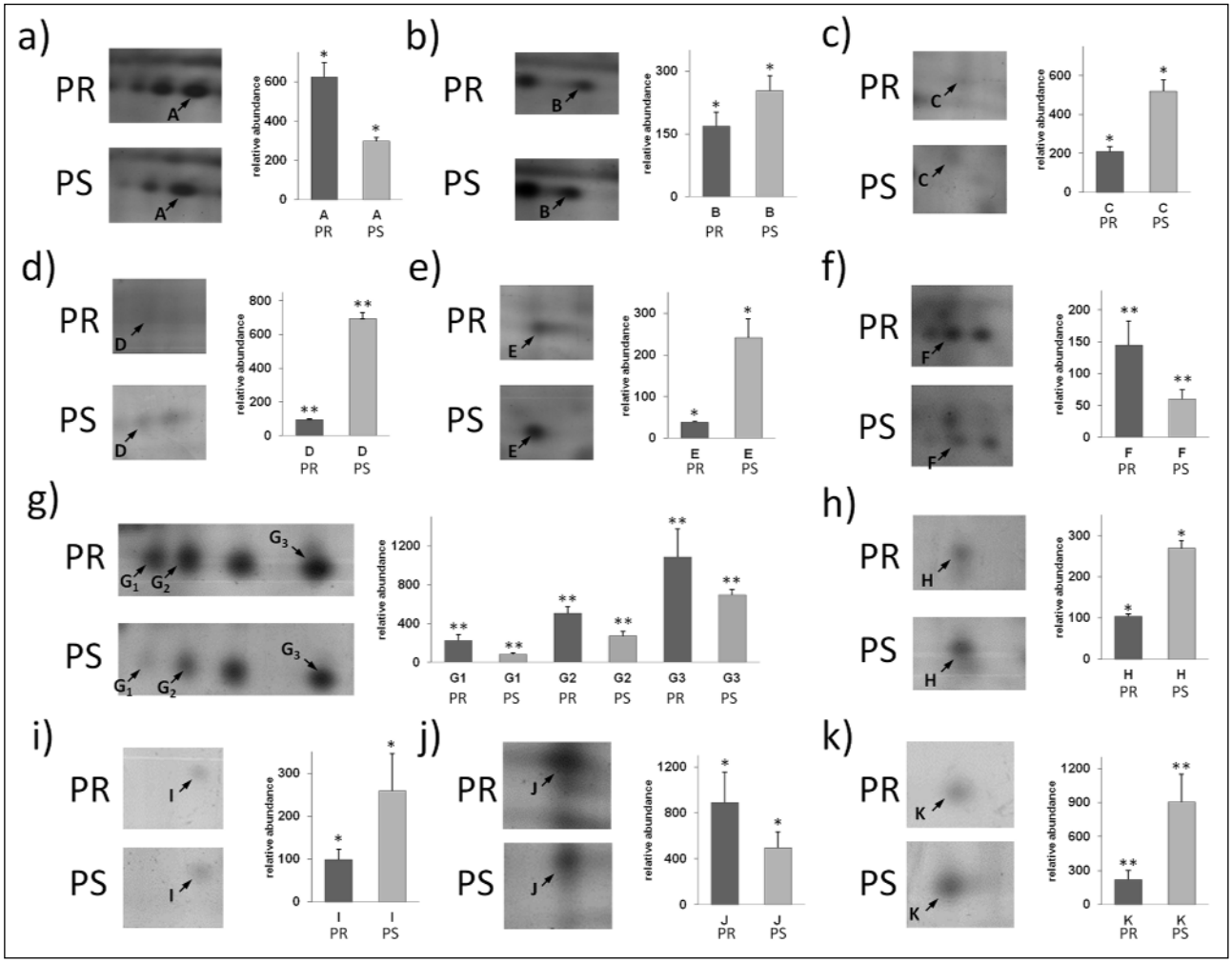

Fig. 3. Differential expression patterns of splenic CD4⁺ T cells proteins between pregnant (PR) and pseudopregnant (PS) mice. Panels from a to k show changes in intensities of identified protein spots and graph of differences in their abundances. With * and ** statistically significant changes in abundance at level P≤0.05 and P≤0.01 were marked.

remaining 12 showed down-regulation. The above-mentioned spots were subjected to identification by PMF. In total, thirteen protein spots were identified, representing 11 distinct proteins. Among identified spots, differences in protein expression in pregnant mice compared to pseudopregnant mice were as follows: ATP synthase subunit beta E (2.10), 40S ribosomal protein (–1.50), F-actin capping protein subunit alpha-1E (–2.50), Malate dehydrogenase, cytoplasmic (–7.19), F-actin capping protein subunit alpha-2 (–6.31), Tropomyosin alpha-3 chain E (2.42), Rho GDP-dissociation inhibitor 2 E (2.63), Rho GDP-dissociation inhibitor 1E (–2.58), Proteasome subunit beta type-4 precursor (–2.64), Carbonic anhydrase 2 E (1.80) and cofilin-1 (–4.11). *Fig. 2* presents the identified (assigned with letters from A to K) and unidentified protein spots (marked with numbers conferred by the PDQuest software SSP). For identified proteins, graphs of differences in abundance and changes in spot intensities are shown in *Fig. 3*. Similarly, detailed information concerning average abundances, fold regulation and significance of differences of the analyzed spots are summarized in *Table 2*.

DISCUSSION

In the present study, we have been able to resolve over average of 350 detected spots, extracted from CD4⁺ T cells from pseudopregnant and preimplantation mice. Unfortunately, 267 protein spots remained unidentified despite repeated analysis. The main reasons responsible for failed identification could be attributed to intrinsic limits of PMF, *e.g.* inability to detect low molecular weight proteins. Numbers of peptides matched to the candidate protein sequence varied from 5 to 40 and the sequence coverage ranged from 13 to 76%. For the majority of the named protein spots resolved in the presented 2-D gel (*Fig. 1*), the shifts between experimental and theoretical molecular masses were noted (*Table 1*). The above-mentioned phenomenon is due to post-translational modifications (PTMs) for *e.g.* phosphorylation, glycosylation and proteolytic cleavage. PTMs result in a shift in the protein's electrophoretic mobility (18). Higher experimental mass values in comparison to the theoretical ones observed for some proteins probably result from

Table 3. A reference list for estrogen-related expression of identified proteins.

CA-II	Carbonic anhydrase 2	Winum JY, Vullo D, Casini A, Montero JL, Scozzafava A, Supuran CT. Carbonic anhydrase inhibitors: inhibition of transmembrane, tumor-associated isozyme IX, and cytosolic isozymes I and II with aliphatic sulfamates. *J Med Chem* 2003; 46: 5471-5477.
CA-I	Carbonic anhydrase 1	Liu CG, Xu KQ, Xu X, *et al*. 17Beta-oestradiol regulates the expression of Na+/K+-ATPase beta1-subunit, sarcoplasmic reticulum Ca2+-ATPase and carbonic anhydrase iv in H9C2 cells. *Clin Exp Pharmacol Physiol* 2007; 34: 998-1004.
H2A.1-H	Histone H2A type 1-H	Dalvai M, Fleury L, Bellucci L, Kocanova S, Bystricky K. TIP48/Reptin and H2A.Z requirement for initiating chromatin remodeling in estrogen-activated transcription. *PLoS Genet* 2013; 9: e1003387.
UMP-CMPK	UMP-CMP kinase	Hirosawa N, Yano K, Suzuki Y, Sakamoto Y. Endocrine disrupting effect of di-(2-ethylhexyl)phthalate on female rats and proteome analyses of their pituitaries. *Proteomics* 2006; 6: 958-971.
ENO1	Alpha-enolase	Malorni L, Cacace G, Cuccurullo M, *et al*. Proteomic analysis of MCF-7 breast cancer cell line exposed to mitogenic concentration of 17beta-estradiol. *Proteomics* 2006; 6: 5973-5982.
ATP5B	ATP synthase subunit beta, mitochondrial precursor	Techritz S, Lutzkendorf S, Bazant E, Becker S, Klose J, Schuelke M. Quantitative and qualitative 2D electrophoretic analysis of differentially expressed mitochondrial proteins from five mouse organs. *Proteomics* 2013; 13: 179-195.
ATP5H	ATP synthase subunit d, mitochondrial	Techritz S, Lutzkendorf S, Bazant E, Becker S, Klose J, Schuelke M. Quantitative and qualitative 2D electrophoretic analysis of differentially expressed mitochondrial proteins from five mouse organs. *Proteomics* 2013; 13: 179-195.
VINC	Vinculin	DePasquale JA, Samsonoff WA, Gierthy JF. 17β-estradiol induced alterations of cell-matrix and intercellular adhesions in a human mammary carcinoma cell line. *J Cell Sci* 1994; 107: 1241-1254.
EZRI	Vinculin	DePasquale JA, Samsonoff WA, Gierthy JF. 17-beta-Estradiol induced alterations of cell-matrix and intercellular adhesions in a human mammary carcinoma cell line. *J Cell Sci* 1994; 107: 1241-1254.
TPM3	Tropomyosin alpha-3 chain	Sukocheva OA, Yang Y, Gierthy JF. Estrogen and progesterone interactive effects in postconfluent MCF-7 cell culture. *Steroids* 2009; 74: 410-418.
ACTG	Actin, cytoplasmic 2	Weisz A, Basile W, Scafoglio C, *et al*. Molecular identification of ERalpha-positive breast cancer cells by the expression profile of an intrinsic set of estrogen regulated genes. *J Cell Physiol* 2004; 200: 440-450.
hnRNP K	Heterogeneous nuclear ribonucleoprotein K	Masuda M, Miki Y, Hata S, *et al*. An induction of microRNA, miR-7 through estrogen treatment in breast carcinoma. *J Transl Med* 2012; 10 (Suppl. 1): S2.
PHB	Prohibitin	He B, Kim TH, Kommagani R, *et al*. Estrogen-regulated prohibitin is required for mouse uterine development and adult function. *Endocrinology* 2011; 152: 1047-1056.
NPM	Nucleophosmin	Skaar TC, Prasad SC, Sharareh S, Lippman ME, Brunner N, Clarke R. Two-dimensional gel electrophoresis analyses identify nucleophosmin as an estrogen regulated protein associated with acquired estrogen-independence in human breast cancer cells. *J Steroid Biochem Mol Biol* 1998; 67: 391-402.
EF2	Elongation factor 2	Blake CA, Kakhniashvili DG, Goodman SR. Mouse anterior pituitary gland: analysis by ion trap mass spectrometry. *Neuroendocrinology* 2005; 81: 229-243.
hnRNP H	Heterogeneous nuclear ribonucleoprotein H	Shao R, Wang X, Weijdegard B, *et al*. Coordinate regulation of heterogeneous nuclear ribonucleoprotein dynamics by steroid hormones in the human fallopian tube and endometrium in vivo and in vitro. *Am J Physiol Endocrinol Metab* 2012; 302: E1269-E1282.
hnRNP A/B	Heterogeneous nuclear ribonucleoprotein A/B	Shao R, Wang X, Weijdegard B, *et al*. Coordinate regulation of heterogeneous nuclear ribonucleoprotein dynamics by steroid hormones in the human fallopian tube and endometrium in vivo and in vitro. *Am J Physiol Endocrinol Metab* 2012; 302: E1269-E1282.
CATH	Cathepsin H precursor	Moulton BC, Khan SA. Progestin and estrogen control of cathepsin D expression and processing in rat uterine luminal epithelium and stroma-myometrium. *Proc Soc Exp Biol Med* 1992; 201: 98-105.
GRP78	78 kDa glucose-regulated protein precursor	Luvsandagva B, Nakamura K, Kitahara Y, *et al*. GRP78 induced by estrogen plays a role in the chemosensitivity of endometrial cancer. *Gynecol Oncol* 2012; 126: 132-139.
GRB2	Growth factor receptor-bound protein 2	Daly RJ, Gu H, Parmar J, *et al*. The docking protein Gab2 is overexpressed and estrogen regulated in human breast cancer. *Oncogene* 2002; 21: 5175-5181.
CH60	60 kDa heat shock protein, mitochondrial precursor	Voss MR, Stallone JN, Li M, Cornelussen RN, Knuefermann P, Knowlton AA. Gender differences in the expression of heat shock proteins: the effect of estrogen. *Am J Physiol Heart Circ Physiol* 2003; 285: H687-H692.
IGHA1	Ig alpha-1 chain C region	Lagerquist MK, Erlandsson MC, Islander U, Svensson L, Holmdahl R, Carlsten H. 17Beta-estradiol expands IgA-producing B cells in mice deficient for the mu chain. *Scand J Immunol* 2008; 67: 12-17.
GAPDH	Glyceraldehyde-3-phosphate dehydrogenase	Schroder AL, Pelch KE, Nagel SC. Estrogen modulates expression of putative housekeeping genes in the mouse uterus. *Endocrine* 2009; 35: 211-219.

glycosylation, whereas lower Mr values are most likely due to proteolytic cleavage.

Complex events underlying maternal immune tolerance involve T cells that are reactive to paternal antigens, which, unfortunately, are rare among other T cell populations and difficult to isolate. Also, these T cells belong to different subpopulations involved in recognition and effector phase of the immune response towards paternal antigens. Although exact specificity of these antigens is not well established, it seems that both T helper and T cytotoxic lymphocytes are aware of their presence (18). On the other hand it has been proved in many experiments that T helper lymphocytes of different subpopulations (Treg, Th1, Th2, Th17) regulate the immune response towards paternal antigens and are disposable for pregnancy maintenance. Moreover, a majority of experiments performed to prove this concept engaged transgenic or inbred mice (19). Although several pregnancy-related mechanisms of immune tolerance were presented, such model experiments leave many questions unanswered, especially those connected with preimplantation events supporting pregnancy tolerance establishment. What is more, in contrast to outbred species, in transgenic or inbred mice the immune balance is very often shifted, which may favor one particular regulatory mechanism. For instance, in mice B6 strain - widely used as a model in experimental reproductive immunology area - Th1 type of response dominates over the Th2 one (20), and hence we adopted a different approach. We used outbred CD-1 mice strain and employed proteomic analysis for an examination of protein expression in the entire population of splenic $CD4^+$ T lymphocytes mice in preimplantation pregnancy.

Peripheral T lymphocytes may be used for examination of gene expression modifications in diverse physiological conditions as they are very sensitive to environmental changes and can serve as biological sensors (21). To asses potential use of T lymphocytes proteome profiling as a tool for monitoring the immune response to early embryo appearance, we compared two groups of mice in preimplantation pregnancy (embryo presence) with pseudopregnant females.

The proteomic map of $CD4^+$ lymphocytes isolated from male transgenic mice created by Kaji *et al.* (12) revealed 255 identified proteins. In our analysis, we identified 63 proteins. Thirty-one proteins from our map were present in the previous one, with 32 additional proteins detected in our examination (*Table 1*). These gene products belong mainly to the group of proteins responsible for metabolism and protein turnover in the cell. Identification of these proteins enriched the proteomic landscape of $CD4^+$ lymphocytes in mice, which now consists of 286 identified proteins. Interestingly, 23 out of 63 proteins identified by us are considered to be estrogen-regulated (*Table 3*). Fifteen of them were not shown in the proteome map of male lymphocytes; therefore, it cannot be excluded that the differences between these two maps (male vs. female) may be a result of estrogen regulation.

The fact that the splenic $CD4^+$ lymphocyte proteome in pregnant mice at 3.5 days after mating differs from the proteome of pseudopregnant animals supports the hypothesis that during the preimplantation pregnancy paternal sperm-derived signals, epididymal fluid and/or signals from the embryo may influence the maternal T-dependent immune response at the periphery. It is a matter of controversy whether specific paternal antigen recognition indeed takes place before implantation (22). Currently, the only described effect of putative paternal antigen recognition by splenic T lymphocytes is an increase of frequency of activated T/T_{reg} cells (7), similarly to significant increase of ^{Treg} frequency after administration of measles virus peptide and food antigen adduct, which led to establishment of oral tolerance. Likewise in the case of measles virus- induced oral tolerance, those inducible T_{regs} have to be antigen-specific, which means they could only suppress antigen-specific response, but could not suppress the effector T cell response triggered by another antigen (23). We do not know if the effects observed in the present study are restricted to the T_{reg} $CD4^+$ cell population or affect the global population of $CD4^+$ cells. Nevertheless, it seems that the presence of paternal signals results in differential regulation of cytoskeleton proteins which are involved in activation and synapse formation in these cells.

Among the proteins that showed altered expression in lymphocytes of pseudopregnant versus pregnant mice, seven of them (cofilin-1, GDIR1 and GDIR2, F actin-capping protein subunit alpha and beta, tropomyosin alpha and 40S ribosomal protein) are key proteins involved in regulation of cell migration and immune synapse formation in T lymphocytes. Expression of cofilin-1, F actin-capping protein subunit alpha-1 and 2, as well as GDIR1, in pregnant mice was significantly decreased in comparison to the pseudopregnant females (*Table 2*). Furthermore, expression of different actin cytoskeleton protein - tropomyosin alpha-3 chain was 2 fold increased. It is possible that migratory activity and cytoskeleton organization are changed in splenic $CD4^+$ lymphocytes of pregnant mice mainly due to the decreased level of cofilin 1. In physiological (chemotaxis of inflammatory cells) and pathological circumstances, cell motility (cancer cells invasion) crucially depends on the reorganization of the actin cytoskeleton (24, 25). Activity and behavior of migrating cells are mediated by internal and external signals, which activate a number of small GTP-binding proteins of the Rho family (26) and thus moderate actin filament reorganization by activation of a number of actin binding proteins (ABPs) (27). For example, the interaction of cofilin (cofilin-1 - non-muscle and cofilin-2 - muscle variant) with monomeric and filamentous actin plays an important role in depolymerization, as well as F-actin severing playing a key role for actin cytoskeleton remodeling (25, 28, 29). On the other hand, the amount of active cofilin is a factor affecting cells' migration abilities (30). The importance of cofilin in leukocyte chemotaxis has been demonstrated in neutrophil-like HL-60 cells and T-cell-like Jurkat cells (31-33). When cofilin expression levels were significantly reduced in these leukocyte-like cell lines, a complete block of chemoattractant-mediated chemotaxis was noted. A decreased amount of cofilin-1 was observed in mouse $CD3^+$ lymphocytes incubated with stress hormones, which was related to diminished migratory activity of cells from stressed animals (34). Moreover, cofilin protein concentration was decreased in T lymphocytes of patients with immune mediated diseases: polycystic ovary syndrome (PCOS) and congenital adrenal hyperplasia (CAH). It is also worth noting that cofilin is responsible for T cell activation with immune synapse formation of naive lymphocytes (35).

In our paper we have shown changes in expression level of two guanine nucleotide dissociation inhibitors (GDIs): GDIμ (GDIR1) and GDI (GDIR2). In pregnant mice, the amount of GDI was decreased, whereas the amount of GDI was increased (*Table 2*). GDIs protect Rho GTPases from degradation in cytosol after geranylgeranylation and deliver Rho proteins to the plasma membrane, where prenylated Rho form of GTP-bound Rho protein associates to the plasma membrane (36). Actin cytoskeleton in lymphocytes is strongly controlled by Rho GTPases: since more than half of known Rho GTPases (14 out of 23), and Rho GDIs (2 out of 3) are expressed in these cells (37). Moreover, GDIα and GDIβ are expressed at high levels in $CD4^+$ lymphocytes (37). Ishizaki with colleagues (38) showed that T lymphocytes of GDIαβ-/- mice exhibited defective chemotaxis. Apparently, regulation of Rho GTPases is extremely important for actin reorganization in T lymphocytes in response to external stimuli and more detailed research should be

performed to elucidate the role of particular GDI in actin cytoskeleton regulation in these cells. Other actin cytoskeleton component - tropomyosin alpha-3 chain (together with beta chain) - is the component of tropomyosin longer form. This protein is a heterodimer, which binds to actin filaments. In non-muscle cells it is implicated in stabilizing cytoskeleton actin filaments. Tropomyosins provide stability to the filaments and regulate association of other actin-binding proteins such as members of ADF/cofilin family to actin filaments. Tropomyosins are competitors of ADF/cofilin for F-actin stabilization, modulating cofilin-actin interaction (39). Another down-regulated protein in pregnant females was F-actin capping protein. The role of this capping protein in lymphocyte motility and activation is not known; however, it was shown that the length and elasticity of actin filaments are ensured by its active binding of barbed actin ends (40). During actin polymerization in the cell, especially to induce movement at the cell periphery, free barbed ends are created and add monomers. Simultaneously, capping proteins, like CapZ, bind barbed ends to stop filament growth (41). Previous studies showed that capping protein is important for the assembly and organization of the actin cytoskeleton *in vivo* (41). Existing data indicate the increase of CapZ (on RNA and protein level) in melanoma cells in comparison to normal melanocytes (42). The decreased amount of 40S ribosomal protein in pregnant mice, also known as laminin-1 binding protein or laminin receptor (LamR) was another important finding. It was shown that LamR is important for both non-tumor (43) and tumor (44) cell migration. Menard et al (45) showed a correlation between overexpression of LamR with increased metastatic ability of breast cancer cells. Venticinque with colleagues observed a decrease of about 90% in NIH 3T3 cell (mice fibroblasts) migration when RPSA/LamR expression was knocked down. What is more, they (43) also showed direct binding of LamR to actin and tubulin, suggesting that LamR connects translational machinery with tubulin, whereas binding of LamR to actin is important for LamR function as surface receptor of laminin. In summary, the observed by us differences in an expression of actin binding proteins in pregnant versus pseudopregnant mice point at decreased turnover of actin and stabilization of actin filaments, which could finally lead to diminished $CD4^+$ lymphocytes migration potential.

Sevenfold down-regulation of cytoplasmic malate dehydrogenase is also worth noting. An increased demand for large quantities of glucose and glutamine and relatively low level of oxidative phosphorylation is characteristic for activated and proliferating lymphocytes. Since cytosolic MDH is engaged in transporting malate from the cytoplasm to mitochondria and, indirectly, in the regulation of the Krebs cycle under hypoaerobic conditions, the decreased level of cytosolic MDH in lymphocytes of pregnant mice suggests lower energy metabolism of these cells. Additionally, a diminished pool of this protein in cellular cytoplasm may restrict proliferation capacity of lymphocytes as the leukemic lymphocytes are characterized by increased levels of this enzyme (46, 47). On the other hand, suppressed proliferative response of $CD4^+$ T cells to primary antigens is characteristic for diseases like diabetes or metabolic stress conditions. T lymphocytes' activation and proliferation was proposed to be modulated by the extracellular levels of adenosine (48). Adenosine elicits its physiological action by ligation to one of four cell- surface receptors regulating immune response or immunosuppression. Adenosine may alter T cell as well as B cell activity, as adenosine-induced cAMP alters IgM production by peripheral blood B cells (49). The type of response mediated by adenosine rely on pattern of expression of adenosine receptors (ARs) on T/B cell surface, which can be regulated by diverted glucose level.

Lymphocyte metabolism in pregnant mice may be also regulated by decreased expression of proteasome subunit beta type-4. This may suggest decreased protein degradation in $CD4^+$ lymphocytes in pregnant mice. This subunit is indispensable for proteasome assembly as one of 7 beta subunits forming beta ring of catalytic 20S proteasome (47). Other two proteins involved in cellular metabolism (*i.e.* ATP synthase subunit beta and carbonic anhydrase) presented slightly increased expression, which may suggest their stabilizing role during pregnancy-associated metabolic changes in lymphocytes.

In conclusion, putative changes in motility of spleen lymphocytes and observed diminished expression of proteins involved in cellular metabolism and protein turnover suggest softening of peripheral lymphocytes activity in temporal close proximity to implantation. However, although the study has gone some way towards enhancing our understanding of maternal recognition of the embryo, many problems need further investigations. It remains to be elucidated if the observed by us proteome of $CD4^+$ lymphocyte in pregnant females is related to peripheral recognition of paternal-derived antigens and whether it is a sign of peripheral priming and induction of specific immunity during pregnancy.

Authors' contributions: A.C. conceived of the study, planned experiments, and wrote the final version of the manuscript. A.L. and A.H. performed 2D gel electrophoresis, image analysis, statistical analysis, and prepared the description of proteomic methods, graphs and tables. M.O. performed mass spectrometry. K.B. and A.K. performed animal experiments, $CD4^+$ lymphocyte isolation and protein extraction, and corrected the final version of the manuscript. D.N. and A.J.M. discussed results concerning cytoskeleton protein expression.

Acknowledgments: This work is supported by Polish National Science Centre grant no. N N311 523940. We thank Lena Romanchuk for her contribution to comparative analysis of protein expression.

Conflict of interests: None declared.

REFERENCES

1. Aluvihare VR, Kallikourdis M, Betz AG. Regulatory T cells mediate maternal tolerance to the fetus. *Nat Immunol* 2004; 5: 266-271.
2. Piccinni MP, Beloni L, Livi C, Maggi E, Scarselli G, Romagnani S. Defective production of both leukemia inhibitory factor and type 2 T-helper cytokines by decidual T cells in unexplained recurrent abortions. *Nat Med* 1998; 4: 1020-1024.
3. Denney JM, Nelson EL, Wadhwa PD, *et al.* Longitudinal modulation of immune system cytokine profile during pregnancy. *Cytokine* 2011; 53: 170-177.
4. Kraus TA, Sperling RS, Engel SM, *et al.* Peripheral blood cytokine profiling during pregnancy and post-partum periods. *Am J Reprod Immunol* 2010; 64: 411-426.
5. Pazos M, Sperling RS, Moran TM, Kraus TA. The influence of pregnancy on systemic immunity. *Immunol Res* 2012; 54: 254-261.
6. Orsi NM, Gopichandran N, Ekbote UV, Walker JJ. Murine serum cytokines throughout the estrous cycle, pregnancy and post partum period. *Anim Reprod Sci* 2006; 96: 54-65.
7. Robertson SA, Guerin LR, Bromfield JJ, Branson KM, Ahlstrom AC, Care AS. Seminal fluid drives expansion of the $CD4^+CD25^+$ T regulatory cell pool and induces tolerance

to paternal alloantigens in mice. *Biol Reprod* 2009; 80: 1036-1045.
8. Thuere C, Zenclussen ML, Schumacher A, *et al.* Kinetics of regulatory T cells during murine pregnancy. *Am J Reprod Immunol* 2007; 58: 514-523.
9. Slawek A, Maj T, Chelmonska-Soyta A. CD40, CD80, and CD86 costimulatory molecules are differentially expressed on murine splenic antigen-presenting cells during the pre-implantation period of pregnancy, and they modulate regulatory T-cell abundance, peripheral cytokine response, and pregnancy outcome. *Am J Reprod Immunol* 2013; 70: 116-126.
10. Grant MM, Scheel-Toellner D, Griffiths HR. Contributions to our understanding of T cell physiology through unveiling the T cell proteome. *Clin Exp Immunol* 2007; 149: 9-15.
11. Delong T, Baker RL, He J, Haskins K. Novel autoantigens for diabetogenic CD4 T cells in autoimmune diabetes. *Immunol Res* 2013; 55: 167-172.
12. Kaji T, Hachimura S, Kaminogawa S. Proteome database of unsensitized CD4 positive T lymphocytes in T cell receptor transgenic mice. *Electrophoresis* 2003; 24: 3433-3444.
13. Lichtenfels R, Rappl G, Hombach AA, *et al.* A proteomic view at T cell costimulation. *PloS One* 2012; 7: e32994.
14. Borro M, Gentile G, Stigliano A, Misiti S, Toscano V, Simmaco M. Proteomic analysis of peripheral T lymphocytes, suitable circulating biosensors of strictly related diseases. *Clin Exp Immunol* 2007; 150: 494-501 .
15. Chae JI, Kim J, Lee SG, *et al.* Quantitative proteomic analysis of pregnancy-related proteins from peripheral blood mononuclear cells during pregnancy in pigs. *Anim Reprod Sci* 2012; 134: 164-176.
16. Chevallet M, Luche S, Rabilloud T. Silver staining of proteins in polyacrylamide gels. *Nature Protoc* 2006; 1: 1852-1858.
17. Westermeier R. Sensitive, quantitative, and fast modifications for Coomassie Blue staining of polyacrylamide gels. *Proteomics* 2006; 6 (Suppl. 2): 61-64.
18. Bonney EA, Shepard MT, Bizargity P. Transient modification within a pool of CD4 T cells in the maternal spleen. *Immunology* 2011; 134: 270-280.
19. Moldenhauer LM, Hayball JD, Robertson SA. Utilising T cell receptor transgenic mice to define mechanisms of maternal T cell tolerance in pregnancy. *J Reprod Immunol* 2010; 87: 1-13.
20. Chen X, Oppenheim JJ, Howard OM. BALB/c mice have more $CD4^+CD25^+$ T regulatory cells and show greater susceptibility to suppression of their $CD4^+CD25^-$ responder T cells than C57BL/6 mice. *J Leukoc Biol* 2005; 78: 114-121.
21. Zhou J, Zhu Z, Bai C, Sun H, Wang X. Proteomic profiling of lymphocytes in autoimmunity, inflammation and cancer. *J Transl Med* 2014; 12: 6. doi: 10.1186/1479-5876-12-6.
22. Erlebacher A, Zhang D, Parlow AF, Glimcher LH. Ovarian insufficiency and early pregnancy loss induced by activation of the innate immune system. *J Clin Invest* 2004; 114: 39-48.
23. He C, Song CH, Cheng L, *et al.* Measles virus-derived peptide/food antigen adducts facilitate the establishment of antigen specific oral tolerance. *J Physiol Pharmacol* 2013; 64: 95-102.
24. Lambrechts A, Van Troys M, Ampe C. The actin cytoskeleton in normal and pathological cell motility. *Int J Biochem Cell Biol* 2004; 36: 1890-1909.
25. Lambrechts A, Van Troys M, Ampe C. The actin cytoskeleton in normal and pathological cell motility. *J Cell Sci* 2009; 122: 305-311.
26. Hall A. Rho GTPases and the control of cell behaviour. *Biochem Soc Trans* 2005; 33: 891-895.
27. Pantaloni D, Le Clainche C, Carlier MF. Mechanism of actin-based motility. *Science* 2001; 292(5521): 1502-1506.
28. Pavlov D, Muhlrad A, Cooper J, Wear M, Reisler E. Actin filament severing by cofilin. *J Mol Biol* 2007; 365: 1350-1358.
29. Kiuchi T, Ohashi K, Kurita S, Mizuno K. Cofilin promotes stimulus-induced lamellipodium formation by generating an abundant supply of actin monomers. *J Cell Biol* 2007; 177: 465-476.
30. Popow-Wozniak A, Mazur AJ, Mannherz HG, Malicka-Blaszkiewicz M, Nowak D. Cofilin overexpression affects actin cytoskeleton organization and migration of human colon adenocarcinoma cells. *Histochem Cell Biol* 2012; 138: 725-736.
31. Hirayama A, Adachi R, Otani S, Kasahara T, Suzuki K. Cofilin plays a critical role in IL-8-dependent chemotaxis of neutrophilic HL-60 cells through changes in phosphorylation. *J Leukoc Biol* 2007; 81: 720-728.
32. Nishita M, Tomizawa C, Yamamoto M, Horita Y, Ohashi K, Mizuno K. Spatial and temporal regulation of cofilin activity by LIM kinase and Slingshot is critical for directional cell migration. *J Cell Biol* 2005; 171: 349-359.
33. Burkhardt JK, Carrizosa E, Shaffer MH. The actin cytoskeleton in T cell activation. *Annu Rev Immunol* 2008; 26: 233-259.
34. Flint MS, Budiu RA, Teng PN, *et al.* Restraint stress and stress hormones significantly impact T lymphocyte migration and function through specific alterations of the actin cytoskeleton. *Brain Behav Immun* 2011; 25: 1187-1196.
35. Samstag Y, Eibert SM, Klemke M, Wabnitz GH. Actin cytoskeletal dynamics in T lymphocyte activation and migration. *J Leukoc Biol* 2003; 73: 30-48.
36. Boulter E, Garcia-Mata R, Guilluy C, Dubash A, Rossi G, Brennwald PJ, *et al.* Regulation of Rho GTPase crosstalk, degradation and activity by RhoGDI1. *Nat Cell Biol* 2010; 12: 477-483.
37. Tybulewicz VL, Henderson RB. Rho family GTPases and their regulators in lymphocytes. *Nat Rev Immunol* 2009; 9: 630-644.
38. Ishizaki H, Togawa A, Tanaka-Okamoto M, *et al.* Defective chemokine-directed lymphocyte migration and development in the absence of Rho guanosine diphosphate-dissociation inhibitors alpha and beta. *J Immunol* 2006; 177: 8512-8521.
39. Bernstein BW, Bamburg JR. ADF/cofilin: a functional node in cell biology. *Trends Cell Biol* 2010; 20: 187-195.
40. Xu J, Casella JF, Pollard TD. Effect of capping protein, CapZ, on the length of actin filaments and mechanical properties of actin filament networks. *Cell Motil Cytoskeleton* 1999; 42: 73-81.
41. Cooper JA, Schafer DA. Control of actin assembly and disassembly at filament ends. *Curr Opin Cell Biol* 2000; 12: 97-103.
42. Sun D, Zhou M, Kowolik CM, *et al.* Differential expression patterns of capping protein, protein phosphatase 1, and casein kinase 1 may serve as diagnostic markers for malignant melanoma. *Melanoma Res* 2011; 21: 335-343.
43. Venticinque L, Jamieson KV, Meruelo D. Interactions between laminin receptor and the cytoskeleton during translation and cell motility. *PloS One* 2011; 6: e15895. doi: 10.1371/journal.pone.0015895.
44. Wewer UM, Taraboletti G, Sobel ME, Albrechtsen R, Liotta LA. Role of laminin receptor in tumor cell migration. *Cancer Res* 1987; 47: 5691-5698.
45. Menard S, Tagliabue E, Colnaghi MI. The 67 kDa laminin receptor as a prognostic factor in human cancer. *Breast Cancer Res Treat* 1998; 52: 137-145.
46. Rabinowitz Y, Dietz AA. Malic and lactic dehydrogenase isozymes of normal and leukemic leukocytes separated on glass bead columns. *Blood* 1967; 29: 182-195.

47. Danis P, Farkas R. Hormone-dependent and hormone-independent control of metabolic and developmental functions of malate dehydrogenase - review. *Endocr Regul* 2009; 43: 39-52.
48. Sakowicz-Burkiewicz M, Pawelczyk T. Recent advances in understanding the relationship between adenosine metabolism and the function of T and B lymphocytes in diabetes. *J Physiol Pharmacol* 2011; 62: 505-512.
49. Sakowicz-Burkiewicz M, Kocbuch K, Grden M, Maciejewska I, Szutowicz A, Pawelczyk T. Impact of adenosine receptors on immunoglobulin production by human peripheral blood B lymphocytes. *J Physiol Pharmacol* 2012; 63: 661-668.

Received: January 27, 2014
Accepted: August 18, 2014

Author's address: Dr. Anna Chelmonska-Soyta, Laboratory of Reproductive Immunology, Ludwik Hirszfeld Institute of Immunology and Experimental Therapy, Polish Academy of Sciences, 12 Weigla Street, 53-114 Wroclaw, Poland
E-mail: soyta@iitd.pan.wroc.pl